Advances in Science and Technology Research Journal

Advances in Science and Technology Research Journal, 2026, 20(4), 402–412
https://doi.org/10.12913/22998624/214170
ISSN 2299-8624, License CC-BY 4.0

Received: 2025.10.07
Accepted: 2026.01.21
Published: 2026.03.01

Ion beam emittance calculations for a disc-shaped hot cavity

Marcin Turek[1]

[1] Institute of Physics, Maria Curie-Skłodowska University, Pl. M. Curie-Skłodowskiej 1, 20-031 Lublin, Poland
E-mail: mturek@kft.umcs.lublin.pl

ABSTRACT

The emittance of ion beams produced by a disc-shaped hot cavity ion source are calculated using a numerical model taking into account the radioactive decay of particles. The changes of beam emittance with the nuclide half-life were studied for the two different cavity shapes, the compact and the flat disc cavity. In both these cases emittance increases with $\tau_{1/2}$. However, the compact ionizer configuration prevails in terms of beam quality for easy-to-ionize substances. The influence of the extraction channel is also under investigation. Although the emittance rises with the extraction opening radius for the both considered shapes it is shown that in the case of the compact ionizer, the saturation of that growth is observed. The scaled efficiency calculations results show that the compact cavity configuration is more tolerant to beam divergence effects due to the increasing extraction channel diameter. This shape was proven to be superior, especially for short-lived nuclides.

Keywords: surface ionization, hot cavity ion sources, ion beam emittance

INTRODUCTION

Particle beams are crucial for a variety of experimental set-ups used in experimental physics, medicine and technology. A lot of effort is made in order to ensure that particle beams of desired current but also other factors like energetic and angular divergence, uniformity and purity could be used e.g. in nuclear spectroscopy, lithography and semiconductor processing, cancer therapy, high energy accelerator physics etc. Numerical simulations are widely used to support and enhance the design of ion beam equipment including ion sources and ion guns [1,2]. Numerical simulations are especially useful in the case extraction and beam forming systems and filters in order to provide, e.g. low emittance or high brightness particle beams [3,4], e.g. of negative ions.

Surface ionization ion sources with hot cavity were developed in 1970s [5,6]. Since that time they were successfully used, e.g. in a variety of isotope separation facilities [7,8]. Their backbone is a semi-opened ionizer usually made of a refractory metal, such as W, Ta or Mo, heated (either ohmically or by electron beams) to a high working temperature (above 2000 K). Usually the ionizer has a form of a tube, however other shapes, like spherical ones could be seen in some devices [9,10]. Even more complicated cavity shapes were proposed as a result of numerical simulations [11]. Usually, the ionizer cavity is connected to an irradiated target (the source of new nuclides) by a transfer system [9,12]. Alternatively, the ionizer wall itself could serve as the irradiated target and the produced nuclides diffuse out directly into the hot cavity [13].

A variety of mathematical models of processes that occur in hot ionizers was considered by different authors over the decades, starting from the models proposed by scientists at JINR, Dubna [14,15]. Other approaches were proposed later on at Western ISOL facilities [16] and focused e.g. on geometrical aspects of a hot cavity [17]. More details and references on this could be found, e.g. in [18]. Most of these models make use of an assumption about a thermal equilibrium between the plasma and the hot walls that emit particle in thermal process. A potential well is then created that prevents the positively charged ions from hitting the walls what could lead to their

neutralization. Multiple collisions of a particle traveling inside the hot cavity amplify the total ionization probability far beyond the limits predicted by the Saha-Langmuir equation.

Several numerical modeling approaches (mostly using the Monte Carlo methods) aiming at the description of the processes taking place inside a hot ionizer could be found in the literature [11,17]. Most of them describe thermal surface ionization in a cavity taking into account the above-mentioned effect of efficiency amplification via multiple particle-wall collisions [18,19]. Several papers focus on the modeling of the release (diffusion) of the newborn nuclides from a target/ionizer walls [20,21]. The effusion in target-ionizer vapor transport connectors was also under investigation [22,23]. A multitude of ionizer shape propositions was put forth in numerical modeling papers, yet the most common is just the tubular one [24,25]. The simple model of the tubular ionizer [19] was also enriched by implementation of an additional effect of electron impact ionization [26]. Later on, spherical or nearly spherical cavities were proposed [27,28]. Several years ago another variation, namely the conical shape were under consideration [29,30]. Calculations of extracted beam emittance were performed for both of these shapes [31,32]. Even more surprisingly, the already mentioned shapes with "spikes'' could be found in the literature [33,34].

Recently, a flat-disc cavity was proposed [35], which should be defined as the special case of a cylindrical ionizer characterized by a length shorter with respect to its radius. Such cavity shape could be regarded as an important and prospective solution, as it could enlarge the number of particle-wall collisions as they move toward an extraction hole. Moreover, such cavity is relatively easy in manufacturing, which cannot be neglected especially in the case of hard-to-machine refractory metals. In [36] it was shown that the flat disc shape could be very effective in the case of stable and long-lived isotopes, especially those which are hard-to-ionize, while the compact shape with small internal ionizer diameter works better for short-lived isotopes, as they spend shorter times until ionized and extracted.

The aim of presented studies was to check the influence of the geometry of the flat cavity and the extraction channel on the produced beam quality. It is also kept in mind that some cavity shapes may be more effective for short-lived isotopes as they reduce the time a nuclide stays in the ionizer (even at the cost of poorer beam quality) while the other shapes are superior rather for stable nuclides. A numerical model enabling intensive simulations of broad spectra of cases seems to be a proper tool that supports the choice of a solution suitable for particular demands or even to find and optimal set of parameters describing the extraction system geometry e.g. for short-lived and hard-to-ionize nuclides.

A short theoretical introduction of emittance as well as the numerical model used for calculations is given for completeness. The results of emittance calculations for values of the inner cavity radius for stable isotopes are shown and discussed. The discussion is enriched by presentation of average number of particle-wall hits and mean time a particle stays inside the cavity. Evolution of ion beam emittance with ionization probability and half-life period for different cavity shape configurations are also under investigation. The influence of the extraction channel geometry, i.e. the extraction opening radius and its length on ion beam quality described by its emittance and the previously used [31,32] concept of scaled efficiency was also studied.

NUMERICAL MODEL

The numerical code calculates trajectories of particles (both neutrals and ions) in the disc-shaped cavity of the ionizer. It derives the total ionization efficiency of an ion source as a ratio of the number primary (non-decayed) ions and the number of all other particles leaving the cavity through an extraction opening. The code was presented in detail in several previous papers, see e.g. [18] and [31]. The simple geometry of the system being considered is shown in Figure 1. It should be kept in mind that the disc-like cavity is a special case of a tubular ionizer geometry in the case when the diameter of the cavity $2r_i$ is larger than its length L. A very simplified extraction system is represented by a single flat extraction electrode having a negative potential V_{ext}. The electrode is placed at the distance $d = 1$ mm from the extraction orifice of the radius r_e. The simulation area discretized uses a 3D rectangular grid (100×400×400 nodes) with the cell sizes $Dx = Dy = Dz = 0.05$ mm.

The electrostatic potential is determined by all fixed electrodes. It is derived by the numerical solving of the Laplace equation via the successive over-relaxation method. The electric field

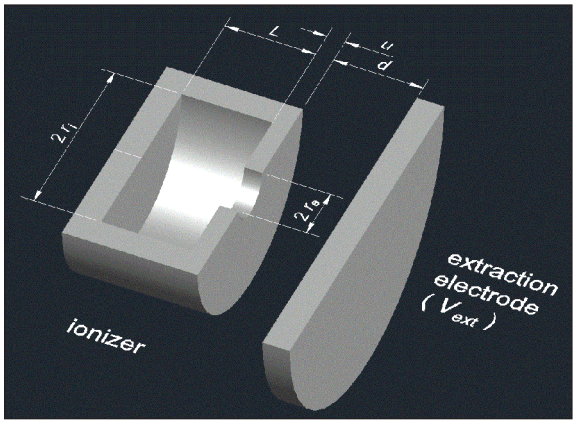

Figure 1. Schematic drawing of the simulated system

acting on charged particles could be easily found as the (negative) derivative of the potential of the previously calculated potential distribution. The value of the pushing forces are derived applying linear interpolation of the six values taken from the closest neighboring grid nodes. The standard 4th order Runge-Kutta formula is used to solve the equations of motion.

Particles are assumed to start from the internal surface of the cavity with purely random direction of their initial velocity. The kinetic energy (and consequently – the value of its velocity) is determined by ionizer temperature T using a simple $E_{kin} = 3\,kT/2$ equation – as the model test, the influence of the cavity geometry and neglects, e.g. forming thermal equilibrium based potential distributions a simple singular delta-like velocity distribution, was chosen, instead of e.g. the more realistic Maxwellian distribution. As in previous papers, for the sake of simplicity particle-particle collisions are neglected and this assumption is well justified as the pressure inside the cavity is very low (of order 10^{-4} mbar [37]) and it means that average distances between particle collisions are above 1 m, much larger than the sizes of the considered cavity.

A crucial feature of the model is the ionization/neutralization mechanism: each particle could be ionized or neutralized during the collision with a hot ionizer wall. The probability of these processes are given by the ionization coefficient β, which is very closely related to another commonly used quantity i.e. an ionization degree:

$$\beta = \alpha/(1+\alpha) \tag{1}$$

The ionization degree is defined as the ratio of the numbers of ions and neutrals that leave the hot surface. This ratio could be estimated using the Saha-Langmuir formula:

$$\alpha = G\exp\left(-\left(V_i - \phi_e\right)/kT\right) \tag{2}$$

where: V_i and ϕ_e are the ionization potential of an travelling atom and the work function of the ionizer material, respectively, and the prefactor G depends on statistic weights of the ion and neutral electronic levels and reflection coefficients.

Due to the fact that each particle spends some time inside the ionizer, mostly due to the sticking to the surface for some time, effects of the radioactive decay should be taken into account. The time that a particle stays on the hot surface could be determined using the Monte Carlo approach for each particle-wall collision:

$$t_{stick} = -\tau_s \ln RND \tag{3}$$

where: t_s is some average sticking time and RND is a normal, i.e. in the range (0,1), random number.

Typical values of t_s for a variety of particle-surface combinations could be found e.g. in [38]. Each primary nuclide (in the considered case it is the nuclide of interest) undergoes decay after some time t_{dec}, which could be derived according to the formula:

$$t_{dec} = -\tau_{1/2} \ln RND \tag{4}$$

where: $t_{1/2}$ is the half-life period of that nuclide.

The code follows trajectories of particles until they pass the extraction and counts the numbers of ions of primary and secondary nuclides (N_{p^+} and N_{s^+}) as well as the number of neutrals (N_{p0} and N_{s0}). The ion source ionization efficiency is defined as the percentage of primary ions among all particle leaving the ion source.

Generally, emittance is a 6-dimensional volume of phase space occupied by particles leaving the ionizer. It is restricted by a 5D surface of some (rather arbitrarily chosen) phase space density [7]. As long as one momentum component (say the z-th one), i.e. all particles, moves in general z direction, one can separate their longitudinal and transversal motion. As the momentum along the beam axis (p_z) is much greater than the transversal one it is justified and comfortable to introduce orbital angles:

$$y' = \frac{p_x}{p_z} \text{ and } y' = \frac{p_y}{p_z} \tag{5}$$

Similarly to that general case, the fractional (or transversal) emittances are defined as the surfaces of the ellipses containing some large part of the ion beam (usually close to, but for obvious reasons not equal to 100%) in the both transversal position-angle subspaces. This paper employed the statistical approach introduced by Chasman and Lapostolle and refined in further papers [39,40]. Accordingly, the root mean square emittance could be calculated as:

$$\varepsilon_{x,rms} = \sqrt{\langle x^2 \rangle \langle x'^2 \rangle - \langle xx' \rangle^2} \text{ and}$$
$$\varepsilon_{y,rms} = \sqrt{\langle y^2 \rangle \langle y'^2 \rangle - \langle yy' \rangle^2} \tag{6}$$

where brackets represent the second central moment of the particle distribution, in the case of symmetric distributions it is just the average. Some authors suggest multiplying that emittance values by the factor 4π to take into account all the particles outside the ellipse.

RESULTS

As the first step, ion beam emittance in the case of stable isotopes was under consideration. The geometry of the ionizer is described by L=1 mm, and r_{ext}=0.5 mm. The extraction electrode potential is V_{ext}= 2 kV and its distance from the extraction hole was chosen as d=1 mm. The ionizer internal diameter was changed from 0.8 mm up to 7 mm. Simulations were done using 100,000 (in the stable isotope case) of test particles of mass 150 a.m.u. The simulation timestep was chosen as 10^{-8} s. The ionizer temperature was set to kT = 0.3 eV.

One can see in Figure 2 that the behavior of emittance is rather complex. For each ionizer diameter it is generally constant for small values of β parameter (i.e. for β smaller than 0.1). For easy-to-ionize substances the beam quality improves, as there are less (on average) number of contacts with wall required in order to achieve ionization. This is confirmed by the data shown in Figure 3, the average number of all hits decreases typically by an order of magnitude in the considered β range. A similar general behavior of $e_{rms}(\beta)$ curves was observed also for conical cavities (see Figure 2 in [32]). The dynamics of that improvement is larger for narrower ionizers (factor 3 for r_i=1.5 mm). It could be seen that the emittance (at the plateau region) is smallest for narrow ionizers (r_i =0.8 mm) and reaches maximum for r_i =1.5 mm. The increase could be due to the fact that some part of the particle reach the extraction from outer regions of the ionizer and have large transversal velocity component, as it was observed in the case of hemispherical [31] and conical [32] ionizers. For wider ionizers (r_i =2 mm and more) beam quality improves, which is rather surprising,

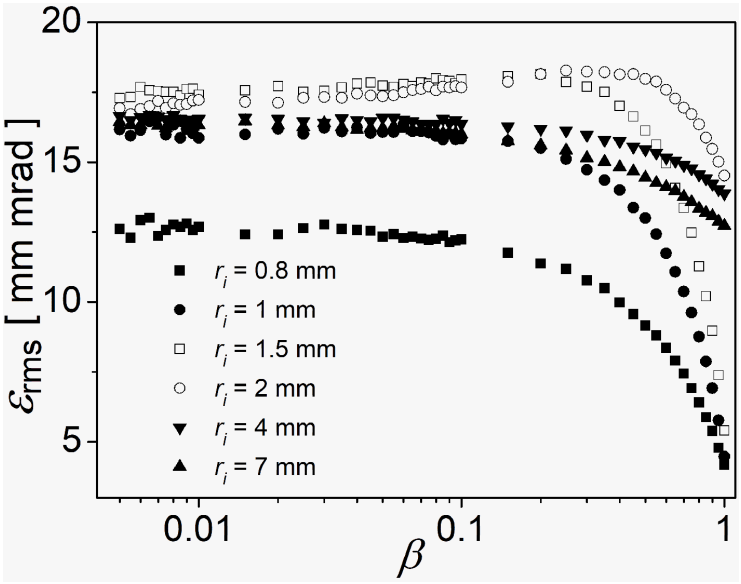

Figure 2. Beam emittance as a function of the ionization coefficient for different values of ionizer radius r_i. The case of stable nuclides

especially bearing in mind that the average number of contacts with ionizer walls simply increases with r_i reaching even several hundreds for r_i=7 mm (see Figure 3). It is observed that this order slightly changes for larger values of β coefficient (curves intersect each other). It should be mentioned here that in the case of stable isotopes, the proposed disc shaped cavity enables ion beams characterized by approximately half the emittance compared to the previously considered cases of hemispherical [31] and conical [32] ionizers. This allows introducing less divergent ion beam into the e.g. beamline system of the ISOL facility.

Evolution of ion beam emittance due to the change of the nuclide halflife was also under investigation. The values of $\tau_{1/2}$ changed in the range from 1 s down to 0.5 μs. Two different cavity shapes were considered, the compact one, characterized by r_i=1 mm, and the flat one for which r_i=4 mm was set. Simulation results are shown in Figure 4. For longer $\tau_{1/2}$ (i.e. larger than 10 ms) the emittance is in the range 15–17 mm mrad for β smaller than 0.1 independently of the ionizer shape. For larger ionization coefficient values, the beam quality improves and this is more distinct in the compact ionizer case. Emittance decreases also for shorter $\tau_{1/2}$ (as $<t>$ becomes comparable to the halflife) and 5 mm rad seems to be limiting value for the compact ionizer, and 12 mm mrad for the flat ionizer. The results for small β value (the flat case) bear large numerical noise despite using larger number of test particles (10^6) as the average time a particle stays in the cavity is much longer than the $\tau_{1/2}$ and the efficiency/extracted current is very low. It should be also mentioned that the order of curves in the case of r_i=1 is the same as in the compact (C) ionizer case described in paper [32]. In the case of the flat ionizer r_i=4 mm one can see again a slight inversion of the curve order and maximal emittance is for $\tau_{1/2}$=10 ms. The same order of $e_{rms}(\beta)$ curves was also observed for β<0.1 in the case of spherical cavity

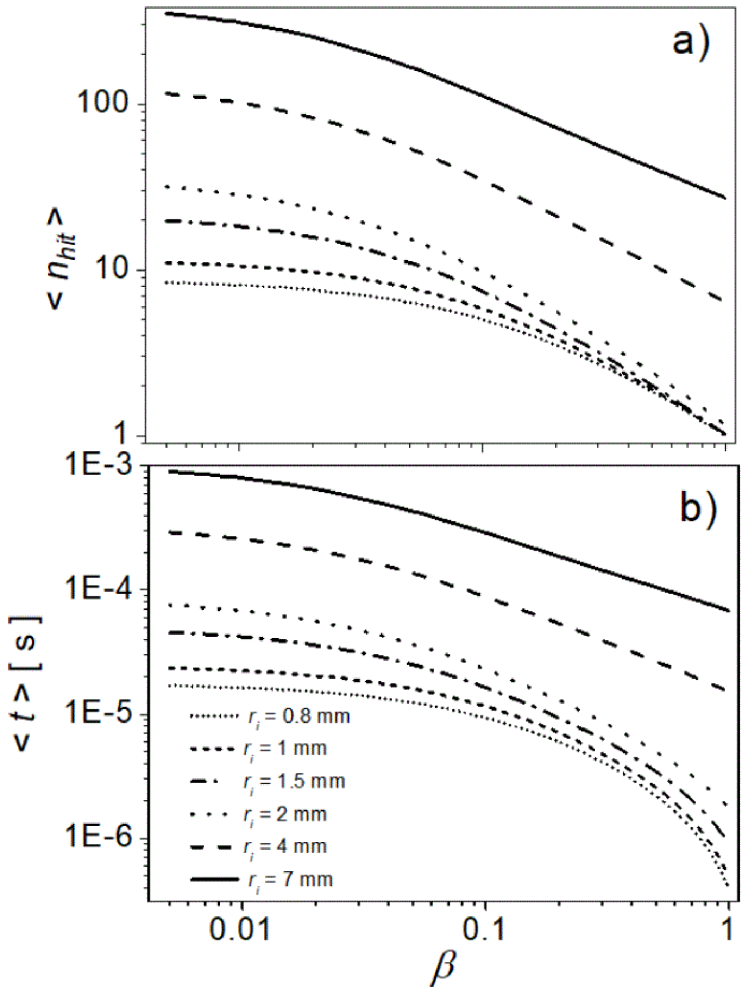

Figure 3. The average number of particle-wall collisions $<n_{hit}>$ (a) and the average time a particle stays inside the cavity $<t>$ (b) for different values of ionizer radius r_i. The case of stable nuclides

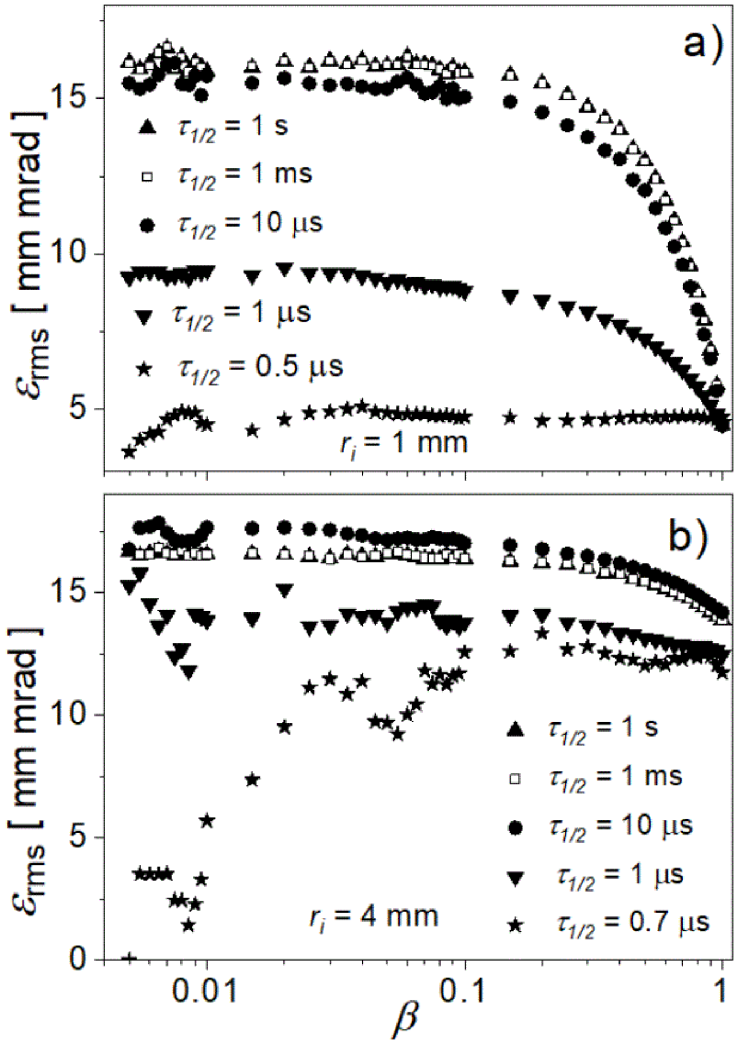

Figure 4. Beam emittance as a function of the ionization coefficient for different values of nuclide halflife $\tau_{1/2}$. The cases of the compact (a) and the flat disc cavity (b)

(configuration A) in [31]. However, it has to be borne in mind that (a) the order was inversed for larger β, (b) the emittance values were ~3 times larger in the case of spherical ionizer.

The influence of extraction channel of the ionizer was also studied. Calculation of the emittance changes due to radius of the extraction opening are presented in Figure 5. As previously, two cavity shape configurations are under consideration r_i=4 mm and r_i=1 mm. The nuclide decay halflife was set as $\tau_{1/2}$=10 ms. Calculations were performed using 10^6 test particles. One can see two families of $\varepsilon_{rms}(\beta)$ curves that behave in a different way for each ionizer configuration. Generally, emittance values achieved for the compact shape are smaller, which is rather obvious due to the fact that the extraction opening radius is limited by r_i. Emittance increases with r_e, the $\varepsilon_{rms}(\beta)$ curves are almost flat for smaller β, then emittance decreases to ~ 5–7 mm mrad in each case. This beam improvement is not observed for very small values of r_e – one can rather see a rise of ε_{rms} with β and intersection of curves. On the other hand, in the case of flat ionizer one can see that for maximal ionization coefficient value (β =1) different values of emittance are achieved, despite the fact that ε_{rms} decreases with β. This might suggest that the emittance in the case of flat ionizer is governed rather by the diameter of the extraction channel while for the compact shape it is limited by the diameter of the ionizer itself.

The next couple of figures (Figures 6a and 6b) present $\varepsilon_{rms}(r_e)$ obtained for β=1. One can see nearly linear increase of ε_{rms} in the case of the flat ionizer (r_e = 2 mm is still much less then the inner ionizer radius) and a kind of saturation of $\varepsilon_{rms}(r_e)$ curve for larger r_e in the case of the compact shape.

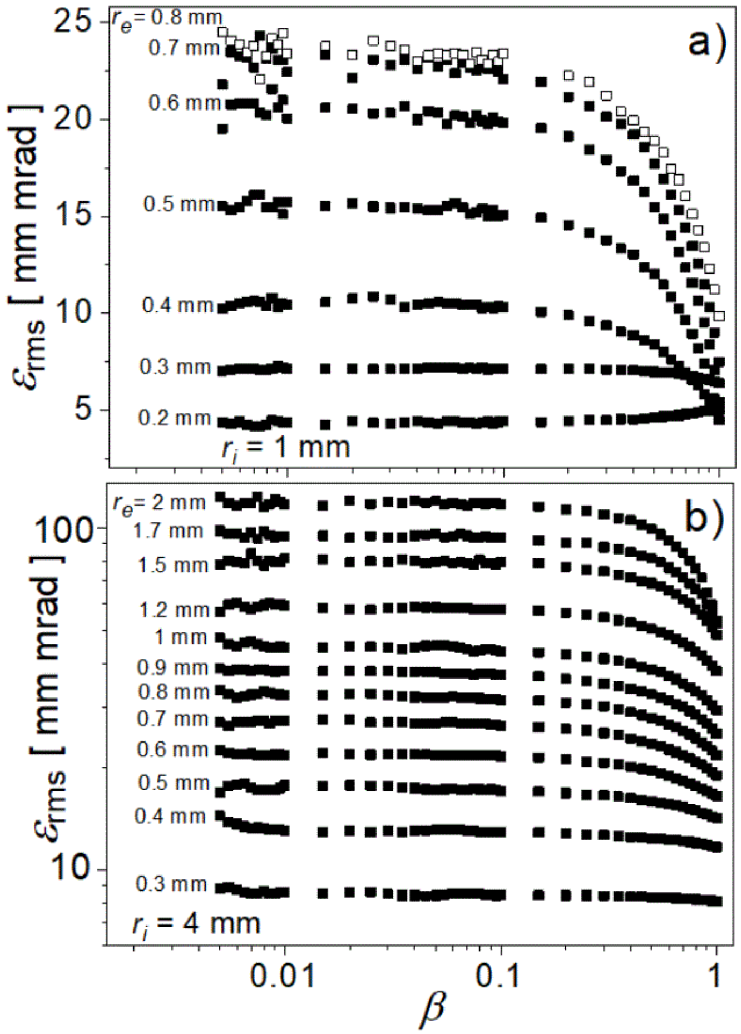

Figure 5. Beam emittance as a function of the ionization coefficient for different values of extraction opening radius r_e. The cases of the compact (a) and the flat disc cavity (b)

Almost linear increase of ε_{rms} was also observed for the compact case of the conical ionizer (compare Figure 5 in [32]), while for the spherical ionizer a saturation of ε_{rms} growth or even surprising decrease of emittance with r_e was seen.

As in the authors' previous papers, scaled efficiency was used, defined as:

$$B = \frac{\beta}{\varepsilon_{rms}^2} \tag{7}$$

by analogy to frequently used beam brightness. Brightness introduces relation between the extracted current an the phase space beam volume, and in the case of scaled efficiency extracted current is replaced by ionization efficiency. One can see that scaled efficiency in both cases decreases with r_e, although the shape of $B(r_e)$ curves is different in both considered cases. In the case of the compact shape one can see that the shape is similar to that observed in the case of compact (C) conical ionizer [32] – one deals with a slow evolution of that magnitude. On the other hand the decrease of the scaled efficiency in the case of the flat ionizer is more rapid, nearly exponential. This is partially due to the fact that the efficiency (not presented here) decreases by more than an order of magnitude in the flat case, while only twice in the compact ionizer case. Similar behavior of scaled efficiency was also observed in the case of compact conical ionizer [32] showing the advantage of minimal size extraction opening also for that design. It should be mentioned here that in the case of spherical or hemispherical ionizer r_e=0.7 mm or above was an optimal choice (see Figure 3 in [31]). To summarize this part – the compact shape with a small diameter extraction opening seems to be the choice suitable for short-living nuclides.

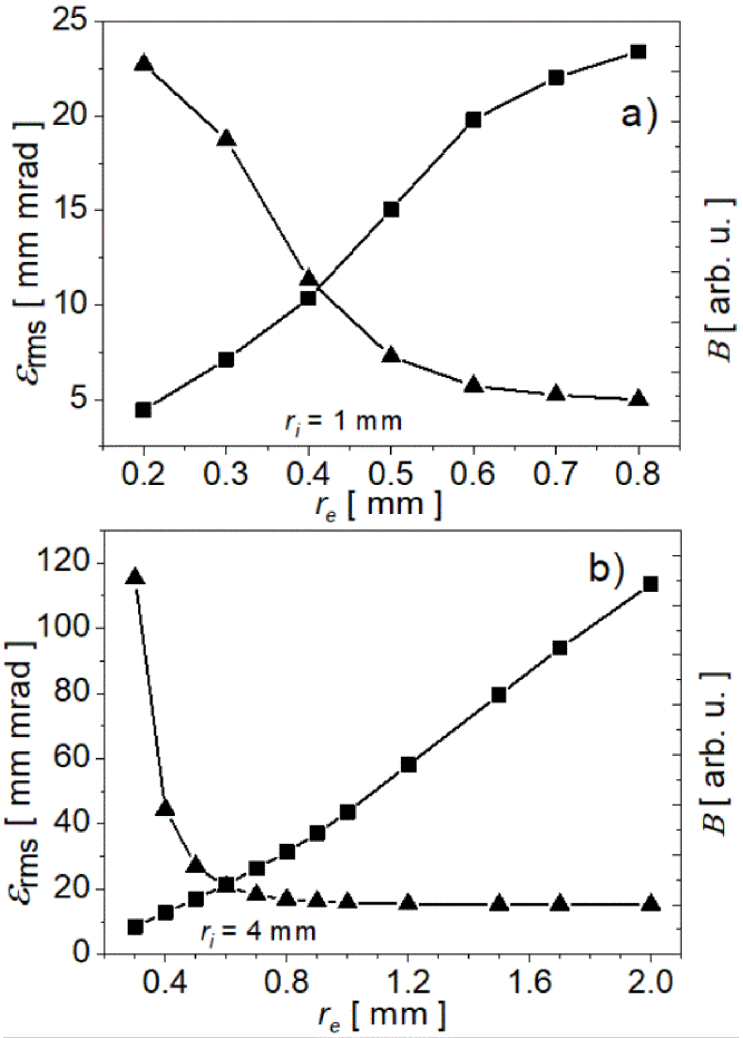

Figure 6. Beam emittance and scaled brightness as functions of the extraction opening radius r_e. The cases of the compact (a) and the flat disc cavity (b)

Another extraction system parameter that usually plays even more important role in forming a low emittance ion beam is the length of the extraction channel. This is because of the fact that the longer is the extraction channel the more effective is the filtering of particles characterized by a large transverse momentum component. Of course, there is another aspect – the longer extraction channel usually leads to less efficient ionization efficiency, mainly as the penetration of the extraction field gets weaker with the increasing extraction channel length. Figure 6 shows the results of the beam emittance and scaled efficiency calculations for u in the range 0.1 mm up to 0.6 mm. The simulations were performed using the same parameter configurations as in the previously considered case, and also for the two cavity geometries (r_i = 1 mm and r_i = 4 mm). The beam emittance decreases with the extraction channel length, as expected. The effect is very similar for the both considered ionizer configurations, i.e. ε_{rms} is reduced approximately by a factor of 2. Again, this is a pattern similar to that obtained in the case of a compact conical ionizer (see Figure 6 in [32]), although one has to mind the lower emittance in the current case as mentioned above.

On the other hand, the evolution of $B(u)$ curves differs for the flat and the compact shape. This is due to the different evolution of ionization efficiency with u for both of these cases. For the flat ionizer ionization the efficiency is reduced by 50% due to the longer extraction channel. This leads to saturation of $B(u)$ curve. In the case of compact ionizer shape the efficiency is not affected much by the change of u and scaled efficiency increases fast. Once again one could see that in the case of fast decaying radioactive nuclides the compact ionizer configuration, especially with a long extraction

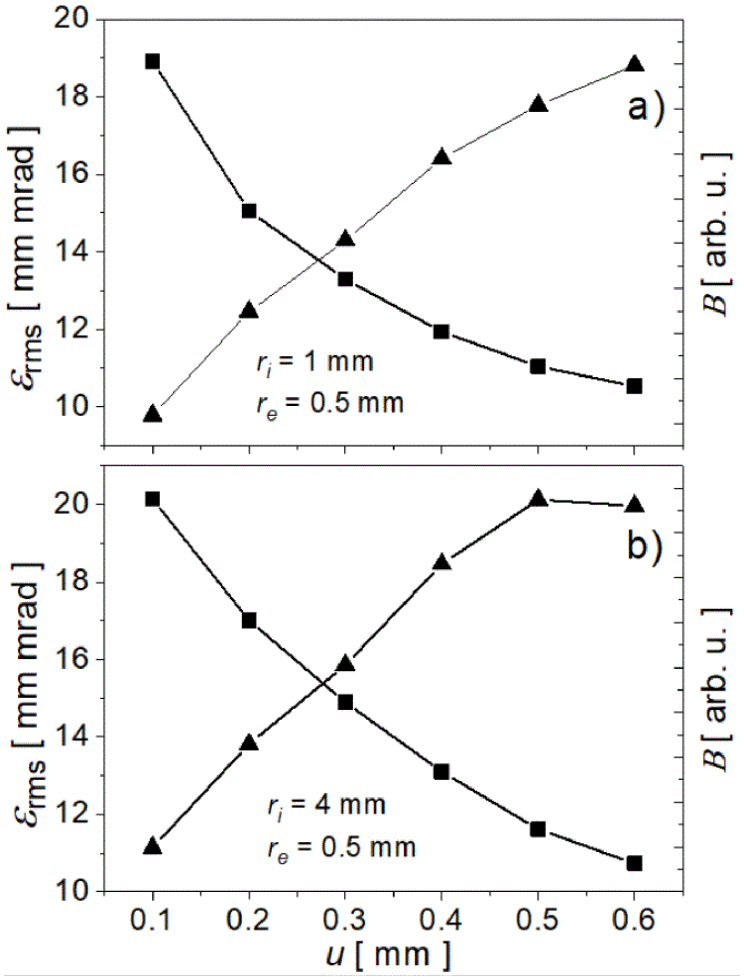

Figure 7. Beam emittance and scaled brightness as functions of extraction channel length u. The cases of the compact (a) and the flat disc cavity (b)

channel prevails, while the flat one works better for stable and hard-to-ionize nuclides (Figure 7).

CONCLUSIONS

Emittance calculations for the ion beams extracted from the disc-shaped cavity ion source based on the numerical model of ionization taking into account the nuclide losses due to radioactive decay was presented in the paper. The beam emittance calculated for stable isotopes exhibits rather complex behavior – it rises with disc ionizer up to certain level and then decreases with r_i. It was shown that $\varepsilon_{rms}(\beta)$ curves intersect each other for larger values of ionization coefficient and the ordering of these curves changes. The evolution of ion beam emittance with the nuclide half-life was also studied for the two different cavity shapes, the compact and the flat disc ionizer. In both these cases the beam emittance increases with $\tau_{1/2}$. However, the improvement of beam quality with rising β is stronger for the compact ionizer configuration.

The impact of the extraction channel geometry on the ion beam quality was under investigation. The ion beam emittance grows with the extraction opening radius for both considered cavity shapes. In the case of the compact ionizer the saturation of $\varepsilon_{rms}(r_{ext})$ curve is observed while r_e approaches r_i. The scaled efficiency dependencies on extraction channel radius help to show the fact that the compact cavity configuration is more tolerant to the effects of increasing r_{ext}. The evolution of emittance and scaled efficiency with the length of the extraction channel u were also tested. It was demonstrated that ε_{rms} decreases with u in both cases; however, in the case of decaying nuclides, the scaled efficiency reaches it maximum for u=0.5 for the flat disc shape, while still increases for the compact ionizer which is superior in the case of short-lived nuclides.

REFERENCES

1. van Kouwen L. Ion emission simulations of the nano-aperture ion source. Imaging and Electron Physics 2019; 212: 307–342. https://doi.org/10.1016/bs.aiep.2019.09.006
2. Cha J-H., S-W. Kim, Lee H-J. A study on beam extraction characteristics of RF and DC filament ion source for high current ion implanters. Applied Science and Convergence Technology 2021; 30(3): 92–94. https://doi.org/10.5757/ASCT.2021.30.3.92
3. Miyamoto K., Nagaoka K., Hatayama A., Hoshino K., Nakano H., Shibata T. and Tsumori K. Study of negative ion beam emittance characteristic using 3D PIC-MCC simulation. J. Phys.: Conf. Ser. 2022; 2244: 012040. https://doi.org/10.1088/1742-6596/2244/1/012040
4. Zhang A., Li D., Xu L., Xiong Z., Zhang J., Peng H. and Luo Q. Simulation and optimization of a miniaturized ion source for a neutron tube. Physical Review Accelerators And Beams 2022; 25: 103501. https://doi.org/10.1103/PhysRevAccelBeams.25.103501
5. Beyer G.J., Herrmann E., Piotrowski A., Raiko V.I., Tyrroff H. A new method for rare-earth isotope separation Nucl. Instrum. Meth. 1971; 96: 437–439. https://doi.org/10.1016/0029-554X(71)90613-6
6. Johnson P.G., Bolson A., Henderson C.M. A high temperature ion source for isotope separators. Nucl. Instrum. Meth. 1973; 106: 83–87. https://doi.org/10.1016/0029-554X(73)90049-9
7. Brown (ed.) I.G. The Physics and Technology of Ion Sources. Wiley, Weinheim, 2004.
8. Kirchner R., On the thermoionization in hot cavities. Nucl. Instrum. Methods Phys. Res. A 1990; 292: 203–208. https://doi.org/10.1016/0168-9002(90)90377-I
9. Alton G.D., Liu Y., Zaim H., Murray S. N. An efficient negative surface ionization source for RIB generation. Nucl. Instrum. Meth. B 2003; 211: 425-435 https://doi.org/10.1016/S0168-583X(03)01365-X
10. Hausladen P.A., Weisser D.C., Lobanov N.R., Fifield L.K., Wallace H.J. Simple concepts for ion source improvement. Nucl. Instrum Meth. B 2002; 190: 402–404. https://doi.org/10.1016/S0168-583X(01)01307-6
11. Maden C., Trinquier A., Fauré A.-L., Hubert A., Pointurier F., Rickli J., Bourdon B. Design of a prototype thermal ionization cavity source intended for isotope ratio analysis. International Journal of Mass Spectrometry 2018; 434: 70–80. https://doi.org/10.1016/j.ijms.2018.09.006
12. Alton G.D., Zhang Y. A fast effusive-flow vapor-transport system for ISOL-based radioactive ion beam facilities. Nucl. Instrum. and Meth A 2005; 539: 540–546. https://doi.org/10.1016/j.nima.2004.11.027
13. Kalinnikov V.G., Gromov K.Ya., Janicki M., Yushkevich Yu.V., Potempa A.W., Egorov V.G., Bystrov V.A., Kotovsky N.Yu., Evtisov S.V., Experimental complex to study nuclei far from the beta-stability line — ISOL-facility YASNAPP-2. Nucl. Instr. and Meth. B 1992; 70: 62–68. https://doi.org/10.1016/0168-583X(92)95910-J
14. Latuszyński A., Raiko V.I. Studies of the ion source with surface-volume ionization. Nucl. Instrum. Meth. 1975; 125: 61–66. https://doi.org/10.1016/0029-554X(75)90553-4
15. Afanas'ev V.P., Obukhov V.A., Raiko V.I. Thermoionization efficiency in the ion source cavity. Nucl. Instrum. Meth. 1977; 145: 533–536. https://doi.org/10.1016/0029-554X(77)90584-5
16. Huyse M., Ionization in a hot cavity. Nucl. Instrum. Methods 1983; 215: 1–5. https://doi.org/10.1016/0167-5087(83)91284-X
17. Latuszyński A., Pyszniak K., Droździel A., Turek M., Mączka D., Meldizon J. Atom ionization process in the thermoionization ion source. Vacuum 2007; 81: 1150–1158. https://doi.org/10.1016/j.vacuum.2007.01.006
18. Turek M. Ionization of isotopes in a hot cavity - Numerical simulations. Vacuum 2014; 104: 1–12. https://doi.org/10.1016/j.vacuum.2013.12.016
19. Turek M., Pyszniak K., Drozdziel A., Sielanko J., Ionization efficiency calculations for cavity thermoionization ion source. Vacuum 2008; 82: 1103–1106. https://doi.org/10.1016/j.vacuum.2008.01.025
20. Mustapha B., Nolen J.A. Optimization of ISOL targets based on Monte-Carlo simulations of ion release curves. Nucl. Instrum. Methods Phys. Res. B 2003; 204: 286–292. https://doi.org/10.1016/S0168-583X(02)01926-2
21. Mustapha B., Nolen J.A., Simulations of effusion from ISOL target/ion source systems. Nucl. Instrum. Methods Phys. Res. A 2004; 521: 59–64. https://doi.org/10.1016/j.nima.2003.11.143
22. Zhang Y., Alton G.D., Monte-Carlo simulation of complex vapor-transport systems for RIB applications. Nucl. Instrum. Methods Phys. Res. B 2005; 241: 947–952. https://doi.org/10.1016/j.nimb.2005.07.154
23. Zhang Y., Alton G.D., Modeling complex vapor-transport systems using Monte-Carlo techniques: Radioactive ion beam applications. J. Vac. Sci. Technol. A 2005; 23: 1558–1567. https://doi.org/10.1116/1.2056553
24. Turek M., Surface ionization of radioactive nuclides - numerical simulations. Acta Phys. Pol. A 2013; 123: 847–850. https://doi.org/1010.12693/APhysPolA.123.847
25. Turek M., Drozdziel A., Pyszniak K., Maczka D., Slowinski B., Simulations of ionization in a hot

cavity surface ion source. Rev. Sci. Instrum. 2012; 83: 023303. https://doi.org/10.1063/1.3685247

26. Turek M., Pyszniak K., Drożdziel A., Influence of electron impact ionization on the efficiency of thermoemission ion source. Vacuum 2009; 83: S260–S263. https://doi.org/10.1016/j.vacuum.2009.01.077
27. Turek M. Modeling of ionization in a spherical surface ionizer. Acta Phys. Pol. A 2011; 120: 188–191. https://doi.org/10.12693/APhysPolA.120.188
28. Turek M. Ionization of short-lived isotopes in spherical hot cavities. Acta Phys. Pol. A 2015; 128: 935–938. https://doi.org/10.12693/APhysPolA.128.935
29. Turek M. Ionisation efficiency in conical hot cavities. Acta Phys. Pol. A 2017; 132: 259–263. https://doi.org/10.12693/APhysPolA.132.259
30. Turek M. Radioactive isotopes ionization in a hot conical cavity (in Polish). Przegląd Elektrotechniczny 2018; 94: 66–69. https://doi.org/10.15199/48.2018.07.16
31. Turek M. Calculations of ion beam emittance for hot cavity ion source. Acta Phys. Pol. A 2015; 128: 931–934. https://doi.org/10.12693/APhysPolA.128.931
32. Turek M. Ion beam emittance for an ion source with a conical hot cavity. Acta Phys. Pol. A 2019; 136: 329–334. https://doi.org/10.12693/APhysPolA.136.329
33. Maden C., Baur H., Fauré A.-L., Hubert A., Pointurier F., Bourdon B. Determination of ionization efficiencies of thermal ionization cavity sources by numerical simulation of charged particle trajectories including space charge. Int. J. of Mass Spectrom. 2016; 405: 39–49. https://doi.org/10.1016/j.ijms.2016.05.013
34. Trinquier A., Maden C., Fauré A.-L., Hubert A., Pointurier F., Bourdon B., Schönbächler M., More than 5% ionization efficiency by cavity source thermal ionization mass spectrometry for U Sub-ng amounts. Analytical Chemistry 2019; 91(9): 6190–6199. mhttps://doi.org/10.1021/acs.analchem.9b00849
35. Turek M. Ionization efficiency in a hot flat disc-shaped cavity. Devices Methods Meas. 2020; 11: 132. https://doi.org/10.21122/2220-9506-2020-11-2-132-139
36. Turek M. Ionization of short-lived nuclides in the hot disc-shaped cavity. Acta Phys. Pol. A 2022; 142: 761–766. https://doi.org/10.12693/APhysPolA.142.761
37. van Duppen P. Isotope separation on line and post acceleration. Lect. Notes Phys. 2006; 700: 37–77. https://doi.org/10.1007/3-540-33787-3_2
38. Eichler B., Huebener S. and Rossbach H., Zentralinstitut fur Kernforschung Rossendorf Report Reports 560 and 561. 1985.
39. Sacherer F. J., RMS Envelope Equations With Space Charge. IEEE Trans. Nucl. Sci. NS-1971; 18: 1105–1107. https://doi.org/10.1109/TNS.1971.4326293
40. Keller R., Sherman J. D., Allison P. Use of a minimum-ellipse criterion in the study of ion-beam extraction systems. IEEE Trans. Nucl. Sci. 1985; 32: 2579–2581. https://doi.org/10.1109/TNS.1985.4333986